

Crystallization and Ionic Associations in Semicrystalline Ionomers

Daniel J. Quiram[†] and Richard A. Register*

Department of Chemical Engineering, Princeton University,
Princeton, New Jersey 08544-5263

Anthony J. Ryan[‡]

Manchester Materials Science Centre,
University of Manchester Institute of Science and
Technology, Manchester M1 7HS, United Kingdom

Received July 15, 1997

Revised Manuscript Received November 17, 1997

Introduction

Ionomers are polymers containing a small amount of bound ionic functionality, typically acid groups neutralized with a metal cation.¹ In bulk, electrostatic forces cause these ionic groups to associate, producing nanometer-size ion-rich aggregates dispersed in a polymer matrix largely depleted of ions. Extensive work has focused on the morphology of ionomers based on amorphous polymers,² such as sulfonated atactic polystyrene. Crystallizable ionomers have been reported on far less, despite their greater commercial importance. The best-known semicrystalline ionomers are based on statistical ethylene–methacrylic acid (E/MAA) copolymers, which DuPont has produced under the trade name Surlyn for over three decades. Early X-ray work³ demonstrated the persistence of ionic aggregates in E/MAA ionomers up to at least 300 °C, and coexistence of polyethylene crystallites and ionic aggregates below the polyethylene freezing point. Later work using resonant small-angle X-ray scattering (SAXS)⁴ confirmed that crystallized specimens exhibit typical polyethylene-like crystallites: lamellae of roughly 5 nm in thickness, separated by somewhat thicker amorphous regions that contain the ionic aggregates.

Despite these observations, little is known about how ionic aggregation and crystallization interact to produce the final structure—how the aggregates are altered during crystallization and how the ionic associations influence the crystallite structure. SAXS data for an E/MAA ionomer presented by Yarusso and Cooper⁵ show that the “ionomer peak”, characteristic of scattering from the aggregates, differs in shape and position between the melt and solid. Modeling of the peak suggested that the aggregates in the solid were smaller and more numerous than in the melt, though later work by Verma *et al.*⁶ found little change. As for how ionic aggregates influence the crystallites, neutralizing E/MAA modestly reduces its degree of crystallinity,⁷ but the effect of ionic associations on the crystal thickness and spacing have not been directly examined.

Here, we investigate the interplay between ionic aggregation and crystallization in sodium-neutralized ionomers via time-resolved simultaneous small- and wide-angle X-ray scattering (SAXS/WAXS). All materi-

als are based on the same E/MAA copolymer, eliminating comonomer content and overall molecular architecture as variables; the molecular features which are varied are the neutralization level and whether the remaining MAA groups are left as the “free” acid or converted to the ethyl ester. Free acid groups in partially neutralized Na⁺ E/MAA ionomers tend to associate with the ionic aggregates;⁸ in the absence of any neutralization, the acid groups exist predominantly as hydrogen-bonded dimers, while the esters do not self- or cross-associate.

Experimental Section

The polymers used here have been described previously.⁸ The E/MAA base resin contains 11.5 wt % MAA, exhibits an intrinsic viscosity of 0.56 dL/g, and has a weight-average molecular mass of 71 Kg/mol, determined by high-temperature light scattering on an esterified derivative. “N_{xx}” indicates an ionomer with *xx* % of the MAA units neutralized by Na⁺, with the remainder as free acid; “Na32E” indicates an ionomer with 32% of the MAA residues neutralized by Na⁺, with the other 68% converted to the ethyl ester; and “H100” indicates the E/MAA base resin.

The SAXS/WAXS experiments were conducted on beamline 8.2 of the Synchrotron Radiation Source in Daresbury, U.K. The beamline, hot stage, and general sequence of experiments and data reduction have been described previously.^{9,10} A 1-m sample-to-detector distance produced a *q* range out to 6 nm^{−1}, capturing the entire ionomer peak. The scattering vector *q* = (4π/λ)sin θ, where λ is the X-ray wavelength (0.154 nm) and 2θ is the scattering angle. The time resolution of the measurements was 6 s. Samples were ramped from room temperature to the 144 °C melt at 20–50 °C/min, held at 144 °C for 1 min, and then cooled at 50 °C/min to the crystallization temperature.

Results and Discussion

Figure 1 shows a typical set of SAXS data (Na83) during crystallization. Time 0 corresponds to when the sample stage first reached the crystallization temperature after cooling from the melt. E/MAA ionomers typically show two SAXS peaks;⁴ the one at lower *q* (position *q*₁^{*}, near 0.5 nm^{−1}) corresponds to scattering between the crystallites, while that at higher *q* (position *q*₂^{*}, near 2 nm^{−1}) corresponds to scattering between the ionic aggregates. After about 1.5 min, the growth of the low-*q* “crystallite” peak becomes noticeable in Figure 1 and is essentially complete by about 4 min. During crystallization, the high-*q* “ionomer” peak moves to higher *q*.

Figure 2 shows how the two SAXS peaks in Na83 change position as the sample is heated, melted, and recrystallized. Assuming a simple paracrystalline model, the average spacing between scattering entities *d* can be found from *d* = 2π/*q*^{*}. For the low-*q* peak, since the crystallites should be roughly lamellar, *q*^{*} is the peak position in a plot of *q*² *I* vs *q*, where *I* is the scattered intensity;¹¹ assuming the ionic aggregates are roughly spherical, then *q*₂^{*} is the peak in a plot of *I* vs *q*. Because both peaks are relatively broad, the choice of *q*² *I* or *I* makes a significant quantitative difference in the *q*^{*} values, but the same trends are present in both.

* To whom correspondence should be addressed.

[†] Present address: The Procter & Gamble Co., Winton Hill Technical Center, Cincinnati, OH 45224.

[‡] Present address: Department of Chemistry, University of Sheffield, Sheffield S3 7HF, U.K.

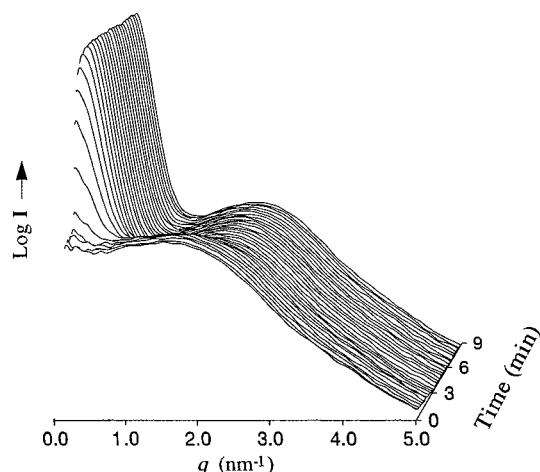


Figure 1. Time-resolved SAXS data for the isothermal crystallization of Na83 at 61 °C, shown on a logarithmic intensity scale. Time 0 corresponds to when the sample stage first reaches 61 °C after cooling from the melt. Each frame shown corresponds to 18 s of data integration.

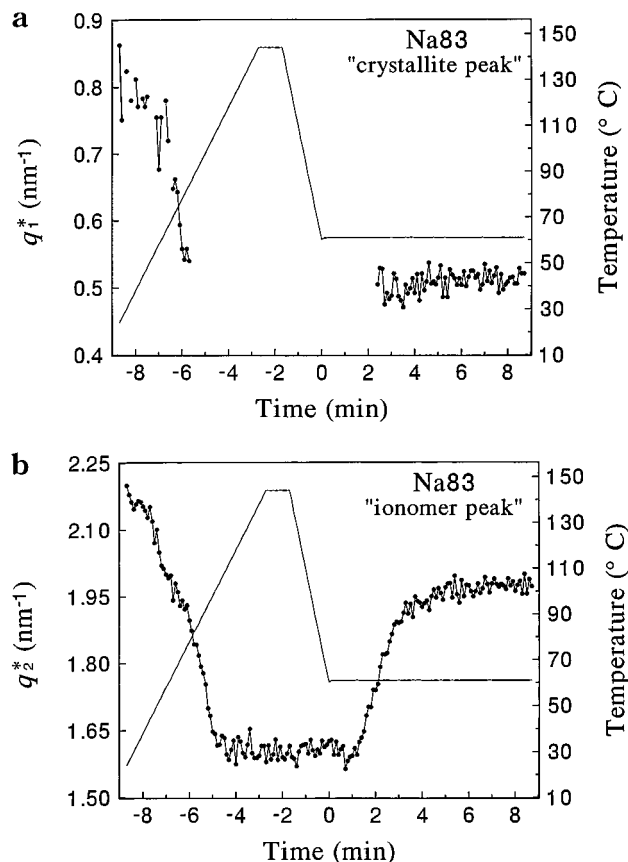


Figure 2. (a) Time evolution of the "crystallite" peak position q_1^* for Na83. The solid line represents the temperature profile (right axis) of the specimen (ending in isothermal crystallization at 61 °C, data of Figure 1), while the points represent q_1^* (left axis). A gap in the points corresponds to molten ionomer. (b) Same as (a), but for the "ionomer" peak position, q_2^* .

As the sample is heated prior to melting, q_1^* decreases. This effect was also noted by Verma⁶ and is typical of all statistical ethylene copolymers: on heating, the smaller and less-perfect crystals melt, leaving fewer and more-widely spaced crystals. During recrystallization, the peak position is essentially constant, indicating that only primary crystallization occurs during the measurement. As for the ionomer peak, it moves

Table 1. Crystallization Characteristics of Selected Ionomers

sample	T_c (°C)	crystallization $t_{1/2}$ (min)	final ϕ_c	melt q_2^* (nm ⁻¹)	solid q_2^* (nm ⁻¹)	Q_2 (solid)/ Q_2 (melt)
Na47	68	1.7	0.15	1.3	2.2	0.82
Na61	64	2.4	0.14	1.6	2.15	0.71
Na83	61	2.1	0.14	1.61	1.98	0.72

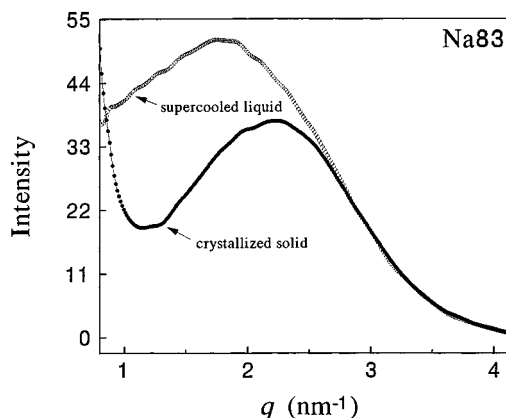


Figure 3. Expanded-scale plot of the SAXS patterns for Na83 at 61 °C, both before (○) and after (●) crystallization. The scattered intensity is given on a linear scale. The thermal density fluctuation background has been subtracted from these data, by fitting the intensity at high q and extrapolating this smooth background to the q range shown here.

progressively to lower q on heating the solid. Once the ionomer has completely melted (at about 100 °C), the peak position does not change detectably on further heating to 150 °C and then supercooling to 61 °C. When the material begins to crystallize, the peak moves to significantly higher q . While the peak appears to move continuously during crystallization, the SAXS patterns at any time are accurately described by a linear combination of the supercooled melt and solid SAXS patterns at 61 °C. The peak observed during crystallization is thus most likely the superposition of two peaks, one arising from crystallized regions of the specimen and one from still-uncrystallized regions of supercooled melt.

Table 1 presents values of q_2^* in the melt and solid at the crystallization temperature (T_c), showing substantial movement of the ionomer peak in all cases. A simple picture of ionomer crystallization might be that the ionic aggregates present in the melt are simply squeezed into the amorphous fraction of the solid, with no other rearrangement. This would indeed shift the peak to higher q , but at T_c the final volume fraction crystallinity ϕ_c obtained from the WAXS data⁹ (Table 1) is only 0.15. Assuming a simple paracrystalline model for the ionomer peak, the shift should scale as $(1 - \phi_c)^{-1/3}$, which predicts an increase of only 6% in q_2^* . Table 1 shows increases of 20–70%, implying that upon crystallization, the ionic groups are redistributed to produce more closely spaced (hence smaller) aggregates. The quantitative validity of a paracrystalline model for such a disordered structure can of course be questioned.¹² However, it seems unreasonable that the large experimental shift in q_2^* , versus the small calculated peak shift, assuming no redistribution of ionic groups, can all be due to departures from simple paracrystallinity.

A related issue is whether the extent of phase separation between ionic and nonionic material remains unchanged during crystallization. Figure 3 shows an expanded-scale plot of the ionomer peak for Na83 at 61

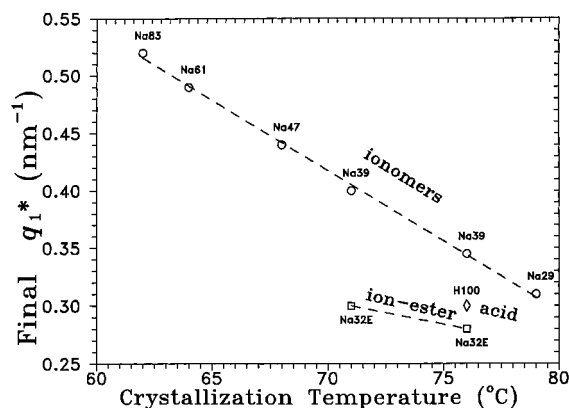


Figure 4. Plot of "crystallite" peak position q_l^* for all specimens examined. Crystallization half-times are comparable (1–7 min) for all points shown, as are volume fractions crystallinity in the final solid (0.13–0.17). Materials are grouped into three categories: (○) "ionomers" (Na x), where unneutralized acid groups are present, (□) "ion-ester" (Na32E), an ionomer where unneutralized acid groups have been converted to ethyl esters, and (◇) "acid", the unneutralized E/MAA base resin.

°C before and after crystallization. The integrated intensity of the ionomer peak—the portion Q_2 of the SAXS invariant that is due to the heterogeneity of the amorphous phase—is smaller in the solid than in the melt. Q_2 is defined as the product $q^2 I$ integrated over the range of q corresponding to the ionomer peak (1.2–4.5 nm⁻¹). In both cases, the relevant electron density difference is that between the ionic aggregates and the surrounding amorphous polymer, essentially amorphous polyethylene; the presence of the crystallites does not influence the scattering from the aggregates, due to the difference in size scales.⁴ For Na83, Q_2 decreases by 28% on crystallization, with similar values for the other ionomers (Table 1), indicating a substantial reduction in the level of phase separation between nonionic and ionic material. While it is possible that the reduction is due to a decrease in the electron density of the aggregates (by incorporation of more polymer), a more likely explanation is that Q_2 drops because crystallization pulls some ionic groups out of aggregates and disperses them into the polymer matrix.

Finally, we examine how the specific associations present in ionomers influence the crystal thickness. Figure 4 shows a plot of the final crystallite peak position q_l^* against crystallization temperature for all the samples studied. The crystallization half-times $t_{1/2}$ determined from the WAXS data⁹ are all between 1 and 7 min, with final volume fractions of crystallinity 0.13 < ϕ_c < 0.17. The data for all the ionomers containing both acid and salt groups lie on a single line to within experimental error; as the neutralization level is increased (and the crystallization temperature is lowered, to hold $t_{1/2}$ roughly constant), the value of q_l^* rises from 0.31 to 0.52 nm⁻¹. As ϕ_c is essentially identical for all samples, the large increase in q_l^* indicates that thinner crystals are produced. Since both neutralization level and crystallization temperature are varied when moving to the left in Figure 4, it is unclear which factor dominates; this point will be returned to below.

Figure 4 also contains data for Na32E, which is similar to Na39 and Na29 except that the remaining free acid groups have been converted to the ethyl esters. The melt viscosity⁸ of Na32E is actually higher than that of Na39, though Na32E crystallizes more rapidly.

The final q_l^* for Na32E is significantly lower (20–25%) than that for Na39 crystallized at the same temperature. The key difference between these two samples is the elimination of the free acid groups, which are known to associate with the ionic aggregates.⁸ By eliminating these associating groups while maintaining essentially the same ion content, significantly thicker crystallites are formed.

Consider the tradeoffs that must occur during crystallization of ionomers based on statistical copolymers. For a given degree of crystallinity, the thickest crystals are obtained by placing the comonomer units (which are unable to enter the crystal lattice) at or near the crystal surface. However, in the ionomer case, putting all the comonomers in a plane at the crystal–amorphous interface would require breaking the majority of the associations (salt–salt, salt–acid, acid–acid). While Figure 3 indicates that some of the ionic associations are broken on crystallization, most are retained. Therefore, the ionomers cannot produce crystals as thick as those produced by a material with an identical content of noninteracting comonomers.

Note also that H100 lies between the curves for the ionomers and Na32E in Figure 4. H100 has the same density of interacting groups as the ionomers, if all such groups (both salt and acid) are counted, but the interactions in H100 are exclusively hydrogen bonds, which are weaker than the salt–salt and salt–acid interactions. The smaller q_l^* , and hence thicker crystals, shown by H100 vs the ionomers, is thus expected; first, hydrogen bonds would be less energetically costly to break upon crystallization, and second, since they are simple pairwise interactions, it is not necessary to break the majority of these associations to localize the comonomer units at or near the crystal–amorphous interface. This trend is consistent with the results of Otocka and Kwei,¹³ who showed that the melting temperatures in ethylene–acrylic acid ionomers were reduced compared with their acid copolymers and suggested that this was likely due to reduced crystallite thickness. By contrast, H100 shows a larger q_l^* (thinner crystals) than Na32E because H100 has 3 times the density of interacting units.

This brings us back to whether the crystals in more heavily neutralized ionomers are thinner because of stronger interactions (salt–salt vs salt–acid) or simply because of the greater undercooling required for crystallization. Figure 4 shows two points for Na39 at different T_c , with $t_{1/2} = 3$ and 7 min; that both points fall equally well on the line with ionomers of different neutralization levels suggests that the main determinant of crystal thickness is crystallization temperature, *not* neutralization level. In other words, the more highly neutralized ionomers form thinner crystals simply because a greater degree of supercooling is needed to effect crystallization at a given rate; salt–salt and salt–acid interactions are of similar effectiveness in limiting the crystallite thickness.

Acknowledgment. The authors would like to thank Dr. John Paul (DuPont-Sabine) for providing many of the ionomers studied here, and for helpful discussions; Dr. Pierre Vanhoorne (Princeton) for providing the balance of the materials; Dr. Dan Wu (DuPont-CR&D) for the high-temperature light-scattering measurement; and Drs. Amit Biswas and Benjamin Hsiao (DuPont-CR&D) for preliminary experiments at the National

Synchrotron Light Source. Financial support for this work came from DuPont Packaging & Industrial Polymers and from the NATO Collaborative Research Grants Program (CRG 951243); beamtime at Daresbury was provided by the EPSRC.

References and Notes

- (1) Jérôme, R.; Mazurek, M. In *Ionomers: Synthesis, Structure, Properties, and Applications*; Tant, M. R., Mauritz, K. A., Wilkes, G. L., Eds.; Blackie Academic and Professional: London, 1997; p 3.
- (2) Grady, B. P.; Cooper, S. L. In *Ionomers: Synthesis, Structure, Properties, and Applications*; Tant, M. R., Mauritz, K. A., Wilkes, G. L., Eds.; Blackie Academic and Professional: London, 1997; p 41.
- (3) Longworth, R.; Vaughan, D. J. *Nature* **1968**, *218*, 85.
- (4) Register, R. A.; Cooper, S. L. *Macromolecules* **1990**, *23*, 318.
- (5) Yarusso, D. J.; Cooper, S. L. *Polymer* **1985**, *26*, 371.
- (6) Verma, R.; Hsiao, B.; Biswas, A. *Polym. Prepr. (Am. Chem. Soc., Div. Polym. Chem.)* **1996**, *37* (1), 415.
- (7) Marx, C. L.; Cooper, S. L. *J. Macromol. Sci., Phys.* **1974**, *B9*, 19.
- (8) Vanhoorne, P.; Register, R. A. *Macromolecules* **1996**, *29*, 598.
- (9) Rangarajan, P.; Register, R. A.; Adamson, D. H.; Fetters, L. J.; Bras, W.; Naylor, S.; Ryan, A. J. *Macromolecules* **1995**, *28*, 1422.
- (10) Bras, W.; Derbyshire, G. E.; Ryan, A. J.; Mant, G. R.; Felton, A.; Lewis, R. A.; Hall, C. J.; Greaves, G. N. *Nucl. Instrum. Methods Phys. Res., Sect. A* **1993**, *326*, 587.
- (11) Russell, T. P. In *Handbook on Synchrotron Radiation*; Brown, G. S., Moncton, D. E., Eds.; North-Holland: New York, 1991; Vol. 3.
- (12) Yarusso, D. J.; Cooper, S. L. *Macromolecules* **1983**, *16*, 1871.
- (13) Otocka, E. P.; Kwei, T. K. *Macromolecules* **1968**, *1*, 401.

MA9710491